SCIENTIFIC REPORTS

OPEN

SUBJECT AREAS:
ELECTRONIC MATERIALS
BATTERIES

Received
3 February 2014

Accepted
14 April 2014

Published
29 April 2014

Correspondence and requests for materials should be addressed to S.Y.Z. (syzheng@usst.edu.cn) or J.H.Y. (jhyang@usst.edu.cn)

High Performance C/S Composite Cathodes with Conventional Carbonate-Based Electrolytes in Li-S Battery

Shiyou Zheng, Pan Han, Zhuo Han, Huijuan Zhang, Zhihong Tang & Junhe Yang

School of Materials Science and Engineering, University of Shanghai for Science and Technology, Shanghai 200093, China.

High stable C/S composites are fabricated by a novel high-temperature sulfur infusion into micro-mesoporous carbon method following with solvent cleaning treatment. The C/S composite cathodes show high Coulombic efficiency, long cycling stability and good rate capability in the electrolyte of 1.0 M $LiPF_6$ + EC/DEC (1 : 1 v/v), for instance, the reversible capacity of the treated C/S-50 (50% S) cathode retains around 860 mAh/g even after 500 cycles and the Coulombic efficiency is close to 100%, which demonstrates the best electrochemical performance of carbon-sulfur composite cathodes using the carbonate-based electrolyte reported to date. It is believed that the chemical bond of C-S is responsible for the superior electrochemical properties in Li-S battery, that is, the strong interaction between S and carbon matrix significantly improves the conductivity of S, effectively buffers the structural strain/stress caused by the large volume change during lithiation/delithiation, completely eliminates the formation of high-order polysulfide intermediates, and substantially avoids the shuttle reaction and the side reaction between polysulfide anions and carbonate solvent, and thus enables the C/S cathode to use conventional carbonate-based electrolytes and achieve outstanding electrochemical properties in Li-S battery. The results may substantially contribute to the progress of the Li-S battery technology.

Lithium-sulfur (Li-S) battery is presently one of the most promising candidates for the next generation lithium batteries because of its relatively high theoretical specific capacity, low cost and environmental friendliness[1,2]. Assuming one S atom can maximally interact with two Li atoms as:

$$S + 2Li^+ + 2e^- \underset{\text{Delithiation}}{\overset{\text{Lithiation}}{\longleftrightarrow}} Li_2S \quad (1)$$

a reversible capacity of 1675 mAh/g can be delivered in theory, which is 10 times higher energy density than that of classical commercial $LiCoO_2$ cathode[3–5]. Actually, at room temperature, sulfur exists mainly in the form of cycloocta sulfur (S_8)[6]. The specific capacity of the S_8 cathode is attained in multi-step lithiation processes upon discharging, involving the high-order polysulfide intermediates (Li_2S_x, $4 \le x \le 8$) and low-order polysulfides of Li_2S_2 and Li_2S in liquid electrolytes, as shown in Eq. (2)–(6)[7,8].

$$S_8 + 2Li^+ + 2e^- \longrightarrow Li_2S_8 \quad (2)$$

$$3Li_2S_8 + 2Li^+ + 2e^- \longrightarrow 4Li_2S_6 \quad (3)$$

$$2Li_2S_6^{2-} + 2Li^+ + 2e^- \longrightarrow 3Li_2S_4 \quad (4)$$

$$Li_2S_4 + 2Li^+ + 2e^- \longrightarrow 2Li_2S_2 \quad (5)$$

$$Li_2S_2 + 2Li^+ + 2e^- \longrightarrow 2Li_2S \quad (6)$$

For practical application, however, Li-S batteries are still plagued by: (i) low active material utilization; (ii) poor cycle life, and (iii) low Coulumbic efficiency. These obstacles arise mainly from insulating nature of sulfur, dissolution of high-order lithium polysulfide intermediates (Li_2S_x, $4 \leq x \leq 8$) in liquid electrolytes, dissolved lithium polysulfides shuttle between anode and cathode, and large volume change during lithiation/delithiation[9–11]. Therefore, how to improve the electronic conductivity, accommodate volume change and avoid the dissolution of polysulfides of the S cathode is crucial for the development of Li-S battery.

Extensive researches have been conducted to overcome these challenges, including optimization of organic electrolytes[12–17], fabrication of sulfur-conductive polymer composites[18–20] and sulfur-carbon-based composites[21–25]. Among them, the most successful technique is the incorporation of S into mesoporous carbon[26]. However, the full electrochemical reversibility is hardly achieved, which leads to a gradual capacity deterioration upon cycling. A reasonable explanation to this problem is that the outward diffusion of polysulfide takes place inevitably during charge and discharge processes[27], *i.e.*, the active material loss could only be alleviated, but not eliminated. This explanation is supported by the use of a non-carbonate solvent-based electrolyte such as ethyl methyl sulphone, dimethoxyethane and dioxolane, tetra(ethylene glycol) dimethyl ether, and polyethylene glycol dimethyl ether, instead of directly using the low-cost classical carbonate-based electrolytes due to the side reaction of dissolved polysulfide anions and carbonate solvents[14,28]. Currently, only few studies on microporous carbon materials as S host were reported because of their less effect in confining polysulfies as compared with mesoporous carbon[29,30]. Recently, we synthesized a microporous carbon-S cathode by infusing small sulfur molecules vapor into MC under vacuum at 600°C showing fairly stable cycling life in Li-S battery using conventional commercial Li-ion battery electrolyte (1.0 M $LiPF_6$ + EC/DEC (1 : 1 v/v))[31,32]. Since only high order polysulfides (LiS_n, $n \geq 4$) are soluble in liquid electrolytes and react with carbonate solvents leading to lower Columbic efficiency and cycling stability, the absent of high-order polysulfides is a key reason for the use of low-cost carbonate-based electrolytes. In this work we fabricated high stable C/S composites *via* a novel sulfur high-temperature (850°C) vacuum-infusion into micro-mesoporous carbon (MC) method following with CS_2 solvent cleaning treatment. The C/S composite cathodes are compatible with conventional carbonate-based electrolytes in Li-S battery and show high Coulombic efficiency, long cycling stability and good rate capability. The structural properties of materials were analyzed by X-ray diffraction (XRD), X-ray photoelectron spectroscopy (XPS), thermogravimetry (TGA), N_2 sorption isotherms, scanning electron microscopy (SEM), energy dispersive X-ray spectrometry (EDS), and transmission electron microscope (TEM). It is believed that the chemical bond of C-S is responsible for the superior electrochemical properties of the C/S composite cathode in Li-S battery. The results here described may substantially contribute to the progress of the Li-S battery technology.

Results

MC was prepared from sucrose according to a reported procedure[30]. The C/S composites were synthesized by infiltration of sulfur into the as-prepared MC under vacuum at 850 °C, that is, sulfur was mixed with MC and sealed in quartz tubes under vacuum, and then the tubes underwent heat treatment at 850°C. Mass ratios of $m_{MC} : m_S = 2 : 1$ and $1 : 1$ were employed to fabricate the C/S composites and denoted as C/S-30 and C/S-50, respectively. The microstructures of the resulting C/S composites were characterized by scanning electron microscopy (SEM) and transmission electron microscope (TEM). **Figure 1** shows the SEM and TEM images of the C/S composites (C/S-30 and C/S-50) and the corresponding energy dispersive X-ray spectrometry (EDS) C and S maps. One can see both C/S-30 and C/S-50 composites have a spherical shape with a particle size of about 300–500 nm. No large bulk S aggregations can be found either in the C/S-30 or in the C/S-50 composite from the TEM images in Figure 1(b) and (f). The EDS intensity spectra shown in **Figure S1** illustrate a relatively quantitative ratio of elemental sulfur and carbon in the selected area for the C/S-30 and C/S-50 composites, respectively; in particular, the elemental mapping images of C and S show that the S maps cover the C maps (see Figure 1(c), (d), (g) and (h)). This clearly indicates that the sulfur is well dispersed in the C/S composites fabricated by sulfur high-temperature vacuum-infusion into MC.

Specific surface area, pore size distribution, and pore volume of MC, C/S-30 and C/S-50 were measured using the N_2 adsorption-desorption isotherms. As shown in **Figure S2**, the MC shows a typical isotherm of type I. The pore sizes (inset in Figure S2) are mainly in the range of around 1.7–6 nm. The MC possesses a high BET specific surface area of 1,650 m^2/g, along with a pore volume of 0.9 cm^3/g. After loading with S, the N_2 sorption isotherms of both C/S-30 and C/S-50 still maintain type I isotherm, but the total amount of the adsorbed N_2 and the pore size are reduced, for instance, the BET specific surface area is reduced from 1,650 m^2/g to around 500 m^2/g

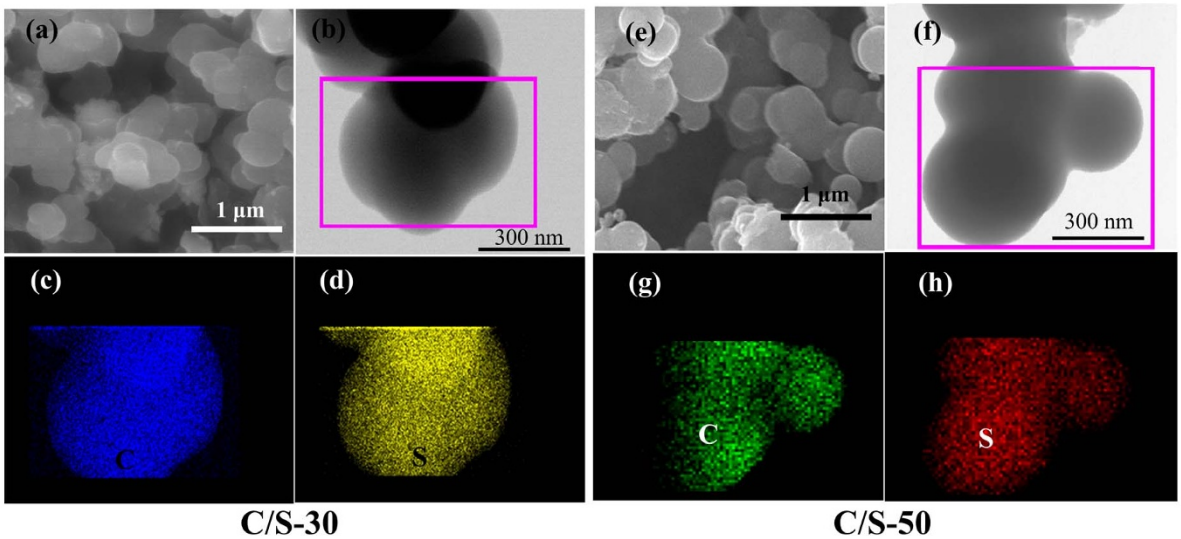

Figure 1 | SEM and TEM images of C/S-30 and C/S-50 composites and the corresponding EDS mapping of C and S.

for the C/S-30 composite and to around 200 m^2/g for the C/S-50 composite, as same time, the pore volume is reduced to 20 and 10% of initial value for the C/S-30 and the C/S-50, respectively. Obviously, either in the C/S-30 or in the C/S-50 composite, there remains pore room that can provide free space for volume change of S/polysulfides during charge and discharge in the Li-S battery.

Electrochemical performances of the C/S composites were investigated as cathode for Li-S batteries in coin cells. The C/S composite was mixed with carbon black and CMC binder to form slurry, and then cast on the current collector of aluminum foil. Lithium metal was used as the counter electrode. The Li-S cells were assembled with electrolyte of 1.0 M $LiPF_6$ (EC/DEC 1 : 1 v/v). **Figure 2** presents the charge and discharge voltage profiles of the C/S-30 and C/S-50 composite cathodes in the 1st, 2nd, 10th, 50th and 100th cycle at current density of 100 mA/g. The discharge/charge curves of the C/S-30 composite cathode show a very short plateau at 2.4–2.5 V (*vs.* Li/Li^+) corresponding to S (S_8) to high-order Li polysulfides and a long plateau at 1.6–1.7 V (*vs.* Li/Li^+) related to the formation of Li_2S_2 and/or Li_2S in the first discharge and only one plateau at 2.0 V (*vs.* Li/Li^+) in the charge (Figure 2(a)). The short plateau at 2.4–2.5 V (*vs.* Li/Li^+) disappeared in the second discharge, which is probably attributed to dissolution of high-order polysulfides. The lithiation capacity is around 1,150 mAh/g in the first cycle, 510 mAh/g in the second cycle, and maintains approximately 500 mAh/g for 100 cycles. The large irreversible capacity in the first charge/discharge cycle is likely due to the dissolution of high-order polysulfide intermediates and side reaction between dissolved polysulfide anions and carbonate solvent, which coincide with the reported result in the literature[30]. As compared to the C/S-30 cathode, the discharge/charge profiles of C/S-50 cathode possesses a relatively longer high-voltage (2.4–2.5 V) plateau in the first discharge and has much larger reversible capacities (Figure 2(b)), which are ascribed to more S_8 in the composite. Either in the C/S-30 or C/S-50 cathode, there exists a relatively lower lithiation voltage in first cycle than that in the following ones, which is mainly attributed to large strain/stress since large volume change requiring a large overpotential, while the strain/stress was reduced in the second lithiation due to introduction of large defects in the electrode and pore size expansion of carbon in the first lithiation, thus reduced the overpotential and shifted the voltage to the high voltage in the second lithiation[33,34]. The voltage of discharge plateau after the initial cycle is relatively lower than that of the S_8/C cathode reported in the literatures. Such a low-voltage feature was previously reported in both carbon-S composites and conductive polymer-S composites synthesized at relatively higher temperature ($\geq$300°C) and attributed to chemical interaction between S and carbon of matrix[21,30]. It is noteworthy, although capacity quick drops take place in the first cycle both for the C/S-30 cathode and for the C/S-50 cathode in Li-S cells with the carbonate-based electrolytes, after then the reversible capacities demonstrate almost no capacity fade with progressive cycling. According to our previous research, it can be deduced that because the resident S (S_8) in the C/S composite is easily dissolved into the carbonate-based electrolyte due to formation high-order polysulfides and/or reacted with carbonate solvent, the resident bonding S plays a key role in the stable C/S composite compatible with the conventional commercial Li-ion battery electrolyte[32,35]. Therefore, we should expect much higher reversible capacities to be obtained for these C/S composite cathodes if the S_8 in the C/S composites can be removed to reduce the irreversible capacity in the first cycle.

The C/S-30 and C/S-50 composites were treated with CS_2 to clean away the resident S_8, and indicated as C/S-30-T and C/S-50-T. The phase components of the C/S composite before and after the treatment of CS_2 were characterized by X-ray diffraction (XRD). **Figure 3** shows the patterns of MC, C/S-30, C/S-50, C/S-30-T and C/S-50-T, respectively. The pristine MC only shows two broad peaks in the range of 20–50° (curve a), demonstrating that MC is an amorphous carbon. For the C/S-30 sample, the peaks belonging to S_8 crystalline phases are almost invisible (curve b). It was reported that at above 850°C, the 99% of crystalline S_8 will be dissociated into short chain sulfur (S_2) and these sulfur small molecules would strongly interact with the surface and form a mono- or few-layered coverage of the matrix surface[36,37]. The XRD falls to detect S peaks in the C/S-30 either because S in pores of carbon is ultra-thin layer or because S is amorphous. After treating with CS_2, the pattern of the C/S-30-T is almost identical to that of the C/S-30, showing only two broad peaks from the porous carbon (curve (c)). As the S content was increased from ~30 to ~50% for the C/S-50 sample, the peaks of the crystalline S are clearly visible in curve (d), which indicates that the small molecular S physically absorbed on the outside of carbon changed back to S_8 when temperature cooling down to room temperature due to high S loading. While the C/S-50 was treated with CS_2, as expected, the peaks belonging to S_8 crystalline phases disappear in the C/S-50-T (curve (e)) sample. The difference in XRD pattern between the C/S-50 and the C/S-50-T demonstrates that the S_8 can be completely cleaned away using CS_2. The specific surface area, pore size distribution, and pore volume of the C/S-30-T and C/S-50-T composites were measured using the N_2 adsorption-desorption isotherms and the results were shown in **Figure S3**. As compared with the samples before treatment, the BET specific surface area and the pore volume are increased to some extension both for the C/S-30-T and C/S-50-T, which is attributed to elimination of the S_8 in the C/S composites.

The electrochemical performances of the C/S-30-T and C/S-50-T composites were also evaluated as cathodes for Li-S batteries in coin cells. The first three charge/discharge profiles of the C/S-50-T electrodes at 100 mA/g are displayed in **Figure 4**(a). As expected, the short plateau at 2.4–2.5 V (*vs.* Li/Li^+) that observed in the C/S-50

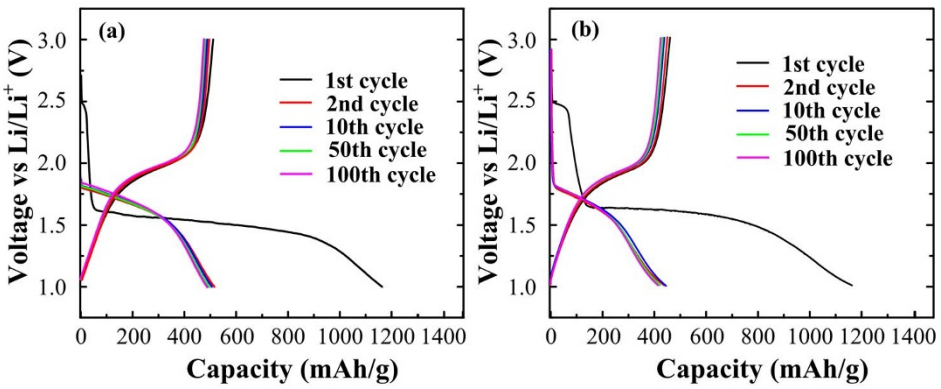

Figure 2 | Discharge/charge voltage profiles of the C/S composite electrodes before CS_2 treatment in the 1st, 2nd, 10th, 50th and 100th cycle at 100 mA/g using the electrolyte of 1.0 M $LiPF_6$ + EC/DEC (1 : 1 v/v): (a) C/S-30, and (b) C/S-50.

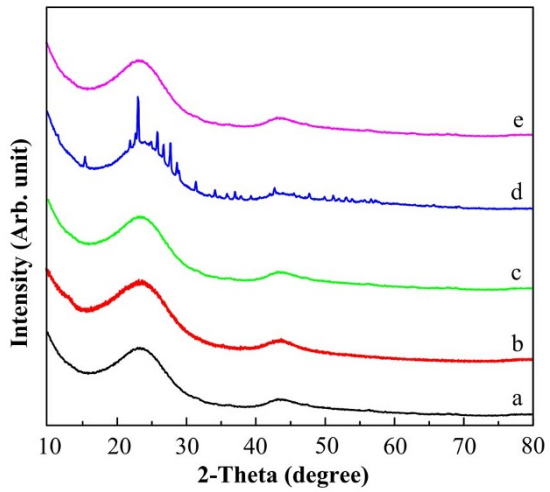

Figure 3 | **XRD patterns of samples: (a) MC, (b) C/S-30, (c) C/S-30-T, (d) C/S-50, and (e) C/S-50-T.**

(before CS_2 treatment, see Figure 2(b)) is almost invisible and only one long plateau at 1.6–1.7 V (*vs.* Li/Li^+) appears in the first discharge for the C/S-50-T electrode. This indicates that the elimination of the S_8 can be manipulated by the simple solvent cleaning, which agrees with the XRD results. Similar to the C/S-50 electrode (shown in Figure 2(b)), the C/S-50-T electrode has only one plateau at 2.0 V (*vs.* Li/Li^+) in the charge and the discharge plateau voltage shifts from 1.6–1.7 V (*vs.* Li/Li^+) in the first cycle to around 1.8 V (*vs.* Li/Li^+) in the second cycle due to relaxation of the strain/stress through expansion of pore size of high surface area MC. The lithiation capacity is around 1,200 mAh/g in the first cycle, 950 mAh/g in the second cycle, and approximately 920 mAh/g in the third cycle for the C/S-50-T cathode, showing high reversible capacity. Although a high reversible capacity can be obtained after the initial cycle, the irreversible capacity of around 250 mAh/g in the first charge/discharge cycle is occurred, which is mainly caused by the porous carbon matrix. We conducted a control experiment by using the as-prepared MC as a cathode, that is, a MC electrode without S was prepared and tested in Li-S cell identical to the fabrication procedure and electrochemical measurements of the C/S composite electrode. The voltage profiles of porous carbon shows that the initial discharge capacity of the MC electrode in the Li-S cell is around 250 mAh/g; after the first cycle, the capacity quickly drops to less than 100 mAh/g in the second cycle and gradually declines with the progressive cycling (**Figure S4**). The initial three-cycle lithiation/delithiation behaviors of the C/S-50-T cathode was also characterized using cyclic voltammetry (CV), displaying in Figure 4(b). As for the C/S-50 electrode without treatment, there exhibit one sharp cathodic peak at about 2.4 V (*vs.* Li/Li^+) along with a board peak at around 1.1 V (*vs.* Li/Li^+) in the first cycle (see **Figure S5**). While for the C/S-50-T, the high-voltage cathodic peak is almost invisible, that is, only one board low-voltage peak can be observed during the cathodic scan. The big difference of the first cathodic scan in CV curves for the C/S-50 before and after treatment can be easily understand because the peak at high voltage of 2.4 V (*vs.* Li/Li^+) is associated to the formation of soluble high-order polysulfides through lithiation of minor resident S_8 on outside surface of porous carbon in the C/S-50, which vanishes in the flowing cycles due to dissolution in electrolyte and/or side reaction between polysulfide anions and carbonate solvent. The low-voltage peak at 1.1 V (starting at 1.8 V (*vs.* Li/Li^+)) is related to the lithiation of the chemical bonding S to Li_2S. It is noteworthy that either for the C/S-50 or the C/S-50-T electrode, the low-voltage peak current near 1.1 V

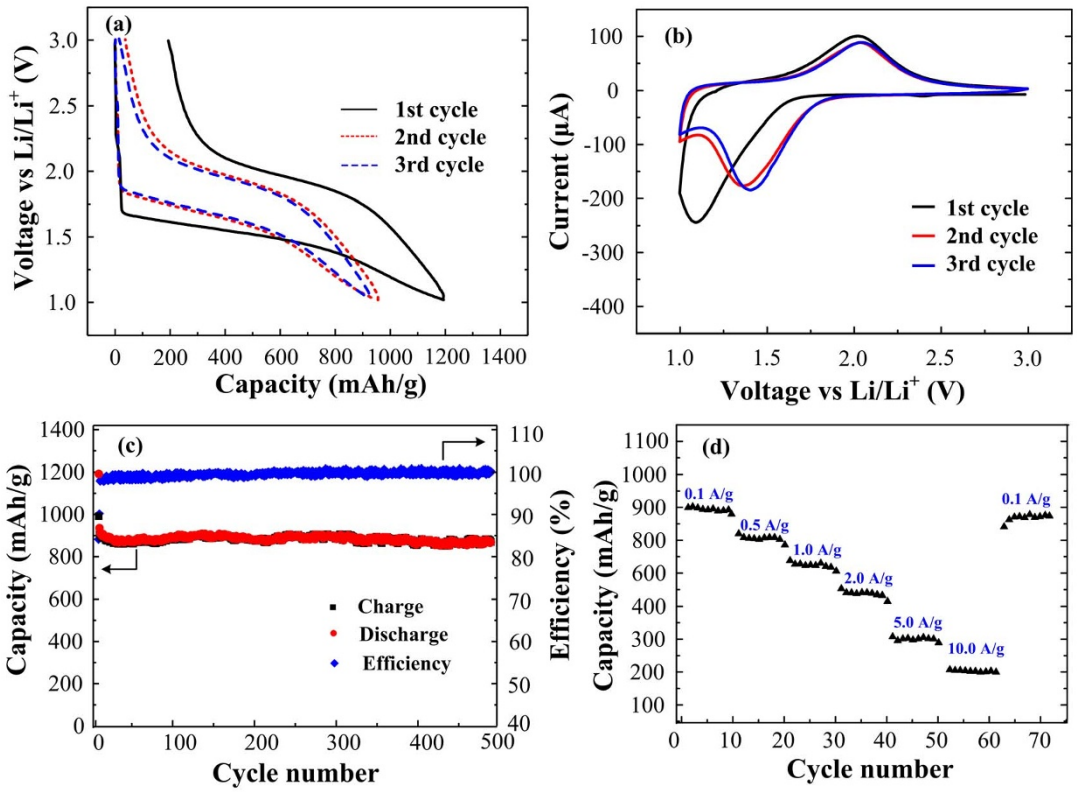

Figure 4 | **Electrochemical properties of the C/S-50-T composite cathode using the electrolyte of 1.0 M $LiPF_6$ + EC/DEC (1 : 1 v/v): (a) Discharge/charge voltage profiles in the first three cycles at a current of 100 mA/g, (b) Cyclic voltammograms in the initial three cycles within the voltage window of 1.0–3.0 V at a scan rate of 0.1 mV/s, (c) Cycling performance and Coulombic efficiency curves, and (d) Rate capability behaviors at different current density from 0.1 A/g to 10.0 A/g.**

(*vs.* Li/Li^+) was reduced and shifted toward more positive direction after the first cycle, which is due to the introduction of large defects in the electrode and pore size expansion of carbon in the first lithiation. For anodic scan, only one peak at 2.0 V (*vs.* Li/Li^+) associating with oxidation of Li_2S. The stable cathodic and anodic current peaks in the first and following scans also demonstrate good cycling stability of the C/S-50-T composite cathode. The CV scan agrees the observed results from the charge/discharge curves. The cycling stability of the C/S-50-T electrode is presented in Figure 4(c), showing high Coulombic efficiency and long cycling stability. Even cycling up to more than 500 cycles, the C/S-50-T cathode retains a capacity of more than 860 mAh/g and the Coulombic efficiency is close to 100% except for the initial few cycles. As compared with the result reported in the literature (Ref. 30), showing a large irreversible capacity of around 350 mAh/g for the cathode in the first cycle, which inevitably requires extra anode to compensate the first-cycle irreversible capacity in practical assembly of Li-S battery, and thus resulting in the reduction of overall capacity for the battery together with the additional cost. While for the C/S-50-T cathode, the first-cycle irreversible capacity is around 200 mAh/g. Moreover, in spite of similar initial reversible capacities for the C/S-50-T cathode and for the reported one in the Ref. 30, quick capacity drops can be observed within 200 cycles and the capacity is around 650 mAh/g after undergoing the 500 cycling charge and discharge for the latter, while for the C/S-50-T cathode, the capacity still retains more than 850 mAh/g, demonstrating much better cycling capability. Similarly, such outstanding cycling stability was also obtained in the C/S-30-T composite cathode (the results shown in **Figure S6**). The long cycling stability and high Coulombic efficiency of C/S-50-T and C/S-30-T cathodes in Li-S cell with the use of carbonate-based electrolyte can be attributed to the elimination of high-order polysulfide intermediates, thus avoiding the shuttle reaction and the side reaction between polysulfide anions and carbonate solvent. The side reaction between polysulfide anions and carbonate solvent has been reported for S_8/C cathode[28], and was confirmed by the above large initial irreversible capacities of the C/S-30 and C/S-50 (without CS_2 washing) composite cathodes. The rate capability behaviors of the C/S-50-T composite electrode in Li-S cell at different current density from 0.1 to 10.0 A/g are shown in Figure 4(d). A reversible capacity of 700 mAh/g can be obtained at a high current density of 1.0 A/g, owing to the good electrical conductivity of MC as matrix to support and bond the highly dispersed S. The value is about 500 mAh/g for 2.0 A/g and 300 mAh/g for 5.0 A/g. A capacity of more than 200 mAh/g can still be delivered even when the current density increases to 10.0 A/g. Moreover, the capacity of approximately 850 mAh/g can be retained when the current density is returned from 10.0 to 0.1 A/g, showing a great merit for an abuse tolerance of Li-S battery with varied current densities.

Discussion

Elemental sulfur has a variety of crystalline and molecular/polymeric forms. At room temperature, sulfur exists mainly in the form of cyclooctasulfur (S_8), as elevating temperature, the cyclo-S_8 molecules can be broken into smaller species, including chain molecules between S_2 and S_7. Further increasing the temperature, the concentration of S_8 steadily decreases along with increase in small sulfur allotropes. Especially, at a temperature of 850°C, short chain (S_2 and S) is the major species, close to 100% of all vapor species. Without further treatment, these small sulfur molecules will recombine to form cyclo-S8 when cooling down. This is supported by the observed S_8 crystalline phases for the C/S-50 composite in the XRD. During the lithiation, the S_8 forms soluble high order polysulfides (LiS_n, $n \geq 4$) in liquid electrolytes, which reacts with carbonate solvents, and thus leading to lower Columbic efficiency and cycling stability. From the electrochemical results above, it is obvious that the C/S composite electrodes, in particular, undergoing CS_2 treatment, have stable, high and reversible capacities together with good rate and cycling capabilities using conventional commercial Li-ion battery electrolyte (1.0 M LiPF6 + EC/DEC (1 : 1 v/v), which demonstrates one of the best electrochemical performance of carbon-sulfur composite cathodes using the carbonate-based electrolyte reported to date. The use of low-cost carbonate-based electrolytes in our C/S composite cathode system is mainly attributed to the absence of the high-order polysulfides, *i.e.*, the chemical bonding between S and the carbon matrix. To further confirm it, the C/S composite materials were further analyzed by X-ray photoelectron spectroscopy (XPS) techniques. **Figure 5** presents the survey scan and S 2p binding energy spectra of the C/S-50-T sample. The S 2p exhibits one strong peak at 164.0 eV along with broad weak centered at 169.0 eV. Further fitting indicates that the strong peak can be split into two peaks for 165.0 and 163.9 eV, respectively, which are assigned to S 2p1/2 and 2p3/2 due to spin orbit coupling, but the binding energies are slightly higher than those of the characteristic peaks of elemental S, indicating that the signals come from the chemical bonding sulfur atoms[38,39]. Moreover, the presence of the broad high binding energy peak positioned between 167 and 172 eV is a direct evidence of the strong interaction of sulfur and carbon[40]. Additionally, a higher sulfur extraction temperatures of the C/S composites were observed during the S content measurements using TGA. The TGA profiles of the C/S-30, C/S-50, C/S-30-T and C/S-50-T are compared in **Figure S7**. It can be seen that the TGA curves of the C/S-30 and C/S-50 composites exhibit two-step feature for the thermal evaporation of S, with the initial weight loss in temperature range of 150 to 250°C following with releasing the rest S at the temperate ranged from 250 to around 500°C. The first weight loss is attributed to the evaporation of S physically covered on the external surface of the MC and the second one in high temperature region is mainly related to strong interaction between S and carbon matrix. For the C/S-30 composite, the weight loss in low temperature range is about 10% and around 22% at the temperate between 250 and 500°C. In the case of the C/S-50 composite, about 21% of S is released within 250°C and the rest S (~27%) can be completely extracted up to 500°C. Undergoing the treatment of CS_2, both the C/S-30-T and C/S-50-T composites show one-step evaporation of S with the onset temperature of 300°C or so and all of S (*ca.* 21% for C/S-30-T and *ca.* 25% for C/S-50-T, respectively) can be evaporated until the temperature reaches to approximate 500°C. The thermal analysis result demonstrates that the part of sulfur (S_8) deposition can be removed by CS_2 at ease but the rest of sulfur has good solvent resistance and remarkable thermal stabilization; on the other hand, it indicates that the S can be indeed stabilized in the C/S composites synthesized through our high-temperature vapor S infu-

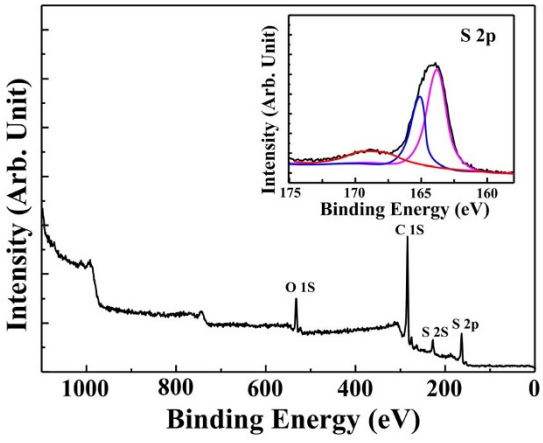

Figure 5 | XPS spectra of C/S-50-T composite, with the inset showing the magnified S 2p spectrum.

sion method, which proves the strong interaction between S and carbon matrix[33].

Obviously, the chemical interaction between S and the carbon matrix plays a key role in the high performance C/S composite cathode, which is attributed to: (i) significantly improving the conductivity of S, effectively buffer the structural strain/stress caused by the large volume change during lithiation/delithiation; (ii) completely eliminating the formation of high-order polysulfide intermediates; (iii) substantially avoiding the shuttle reaction and the side reaction between polysulfide anions and carbonate solvent, and thus enabling the C/S composite cathode to use conventional carbonate-based electrolytes and resulting in exceptional electrochemical properties in Li-S battery.

In summary, the present work demonstrates clearly that highly stable C/S composite materials were synthesized by infusing S into micro-mesoporous carbon at a temperature of 850°C following with solvent cleaning. The C/S composite cathode in Li-S cell with a conventional carbonate-based electrolyte (1.0 M $LiPF_6$ + EC/DEC (1 : 1 v/v)) shows almost 100% of Coulombic efficiency and provides capacity of more than 860 mAh/g without noticeable capacity decline for 500 cycles. The superior electrochemical properties of the C/S composite cathode is attributed to the S chemical interaction with the carbon matrix, which can significantly improve the conductivity of S, effectively buffer the structural strain/stress caused by the large volume change during lithiation/delithiation, and completely eliminate the formation of high-order polysulfide intermediates, and substantially avoid the shuttle reaction and the side reaction between polysulfide anions and carbonate solvent. We believe that the results here described may substantially contribute to the progress of the Li-S batteries technology.

Methods

Synthesis of micro-mesoporous carbon (MC). MC was synthesized according to a reported procedure[30]. Sucrose was dissolved in 6.0 M sulfuric acid to form a mass fraction of 5% sucrose solution, which was placed in a round bottom flask and refluxed at 120 °C for 10 h to yield a dark brown precursor. The precursor was filtered, washed by water, air-dried at 100 °C overnight to form a solid. Then the solid product was calcined under argon at 1000 °C for 2 h, with a heating rate of 10°C/min.

Preparation of C/S composite. The C/S composite was prepared by infiltration of sulfur into the MC under vacuum. In this work, mass ratios of $m_{MC} : m_S = 2 : 1$ and 1 : 1 were employed to fabricate C/S composite and denoted as C/S-30 and C/S-50, respectively. First, the prepared MC and the sublimed sulfur (Sigma-Aldrich) were mixed by ground milling, then the mixture was sealed in an evacuated quartz tube, heated up to 850 °C at a rate of 10 °C/min, kept at this temperature for 5 h and cooled down to room temperature. The as-prepared C/S composites were treated with CS_2 for no less than three times, and the resulting samples were dried in vacuum oven at 100 °C for 2 h, indicated as C/S-30-T and C/S-50-T. The sulfur content of the preparing C/S composites were determined by thermogravimetric analysis (TGA) on a Netzsch STA 449 F1, Germany, with a heating rate of 10°C/min, and high purity Ar as the purge gas.

Structural characterization. X-ray diffraction (XRD) patterns were recorded on Rigaku D/max 2400, Japan, with Cu Kα radiation in the 2-Theta range from 10–80°. X-ray photoelectron spectroscopy (XPS) was carried out on a RBD upgraded PHI-5000C ESCA system (Perkin Elmer) with Mg Kα radiation (1253.6 eV). N_2 adsorption-desorption isotherms were measured using a Micromeritics ASAP 2020 Analyzer (USA). Specific surface areas were calculated using the Brunauer- Emmett-Teller (BET) model, and the pore size distributions were evaluated using the Barrett-Joyner-Halenda (BJH) model. Scanning electron microscopy (SEM) images were obtained on a Hitachi S-4700 (Japan) operating at 10 kV. The transmission electron microscope (TEM) samples were examined in a JEOL (Japan) 2100F field emission TEM equipped with an energy dispersive X-ray spectrometry (EDS).

Electrochemical measurements. The C/S composites were mixed with acetylene black and sodium carboxymethyl cellulose binder in a weight ratio of 80 : 10 : 10, with distilled water as a dispersant. The slurry was coated on an aluminum foil to obtain a film with approximately 80 μm thickness and dried in a vacuum oven at 100°C overnight. The active material loading was around 1 mg/cm^2. The half cells were assembled in a glove box filled with high pure Ar. Lithium metal was used as the counter electrode and reference electrode. The separator was microporous polypropylene Celgard®3501 (Celgard, LLC Corp., USA). The electrolyte was 1.0 M $LiPF_6$ in a mixture of ethylene carbonate/dimethyl carbonate (EC/DEC, 1 : 1 v/v). The charge and discharge performances of the half-cells were tested with using Arbin battery test station (BT2000, Arbin Instruments, USA) and potential range was controlled between 1.0 and 3.0 V at ambient temperature. The specific capacity was calculated on the basis of the active S material obtained from TGA measurement. The cyclic voltammetry (CV) measurement was conducted with a Gamry Reference 6000 (Gamry Co., USA) at a scan rate of 0.1 mV/s.

1. Kolosnitsyn, V. S. & Karaseva, E. V. Lithium-sulfur batteries: problems and solutions. *Russ. J. Electrochem.* **44**, 506–509 (2008).
2. Zhang, Y. *et al.* Development in lithium/sulfur secondary batteries. *Open Mater. Sci. J.* **5**, 215–221 (2011).
3. Herbert, D. & Ulam, J. Electric dry cells and storage batteries. *U. S. Pat.* 3043896 (1962).
4. Peled, E. *et al.* Rechargeable lithium-sulfur battery. *J. Power Sources* **26**, 269–271 (1989).
5. Bruce, P. G. *et al.* Li-O_2 and Li-S batteries with high energy storage. *Nat. Mater.* **11**, 19–29 (2012).
6. Meyer, B. Elemental Sulfur. *Chem. Rev.*, **76**, 367–388 (1976).
7. Ji, X. & Nazar, L. F. Advances in Li–S batteries. *J. Mater. Chem.* **20**, 9821–9826 (2010).
8. Manthiram, A. *et al.* Challenges and prospects of lithium-sulfur batteries. *Acc. Chem. Res.* **46**, 1135–1143 (2013).
9. Barchasz, C. *et al.* Lithium/sulfur cell discharge mechanism: an original approach for intermediate species identification. *Anal. Chem.* **84**, 3973–3980 (2012).
10. Scrosati, B. *et al.* Lithium-ion batteries: a look into the future. *Energy Environ. Sci.* **4**, 3287–3295 (2011).
11. Yang, Y. *et al.* Nanostructured sulfur cathodes. *Chem. Soc. Rev.* **42**, 3018–3032 (2013).
12. Yuan, L. *et al.* Improved dischargeability and reversibility of sulfur cathode in a novel ionic liquid electrolyte. *Electrochem. Commun.* **8**, 610–614 (2006).
13. Jung, Y. & Kim, S. New approaches to improve cycle life characteristics of lithium-sulfur cells. *Electrochem. Commun.* **9**, 249–254 (2007).
14. Zhang, S. S. Improved cyclability of liquid electrolyte lithium/sulfur batteries by optimizing electrolyte/sulfur ratio. *Energies* **5**, 5190–5197 (2012).
15. Suo, L. *et al.* A new class of solvent-in-salt electrolyte for high-energy rechargeable metallic lithium batteries. *Nat. Commun.* **4**, 1481 (2013).
16. Aurbach, D. *et al.* On the surface chemical aspects of very high energy density, rechargeable Li-sulfur batteries. *J. Electrochem. Soc.* **156**, A694–A702 (2009).
17. Chen, S. *et al.* Exceptional electrochemical performance of rechargeable Li-S batteries with a polysulfide-containing electrolyte. *RSC Adv.* **3**, 3540–3543 (2013).
18. Fanous, J. *et al.* Structure-related electrochemistry of sulfur-poly(acrylonitrile) composite cathode materials for rechargeable lithium batteries. *Chem. Mater.* **23**, 5024–5028 (2011).
19. Sun, M. *et al.* Nano-wire networks of sulfur-polypyrrole composite cathode materials for rechargeable lithium batteries. *Electrochem. Commun.* **10**, 1819–1822 (2008).
20. Wang, J. *et al.* A novel conductive polymer-sulfur composite cathode material for rechargeble lithium batteries. *Adv. Mater.* **14**, 963–965 (2002).
21. Lai, C. *et al.* Synthesis and electrochemical performance of sulfur/highly porous carbon composites. *J. Phys. Chem. C* **113**, 4712–4716 (2009).
22. Ji, L. *et al.* Porous carbon nanofiber-sulfur composite electrodes for lithium/sulfur cells. *Energy Environ. Sci.* **4**, 5053–5059 (2011).
23. Jayaprakash, N. *et al.* Porous hollow carbon@sulfur composites for high-power lithium-sulfur batteries. *Angew. Chem. Int. Ed.* **50**, 5904–5908 (2011).
24. Weng, W. *et al.* Ultrasound assisted design of sulfur/carbon cathodes with partially fluorinated ether electrolytes for highly efficient Li/S batteries. *Adv. Mater.* **25**, 1608–1615 (2013).
25. Liang, C. *et al.* Hierarchically structured sulfur/carbon nanocomposite material for high-energy lithium battery. *Chem. Mater.* **21**, 4724–4730 (2009).
26. Ji, X. *et al.* A highly ordered nanostructured carbon-sulphur cathode for lithium-sulphur batteries. *Nat. Mater.* **8**, 500–509 (2009).
27. Xu, R. *et al.* Role of polysulfides in self-healing lithium-sulfur batteries. *Adv. Energy Mater.* **3**, 833–838 (2013).
28. Gao, J. *et al.* Effects of liquid electrolytes on the charge-discharge performance of rechargeable lithium/sulfur batteries: electrochemical and in-situ X-ray absorption spectroscopic studies. *J. Phys. Chem. C* **115**, 25132–25137 (2011).
29. Sun, H. *et al.* A composite material of uniformly dispersed sulfur on reduced graphene oxide: Aqueous one-pot synthesis, characterization and excellent performance as the cathode in rechargeable lithium-sulfur batteries. *Nano Res.* **5**, 726–738 (2012).
30. Zhang, B. *et al.* Enhancement of long stability of sulfur cathode by encapsulating sulfur into micropores of carbon spheres. *Energy Environ. Sci.* **3**, 1531–1537 (2010).
31. Guo, J. *et al.* Sulfur-impregnated disordered carbon nanotubes cathode for lithium-sulfur batteries. *Nano Lett.* **11**, 4288–4294 (2011).
32. Zheng, S. *et al.* In situ formed lithium sulfide/microporous carbon cathodes for lithium-ion batteries. *ACS Nano* **7**, 10995–11003 (2013).
33. Kasavajjula, U. *et al.* Nano- and bulk-silicon-based insertion anodes for lithium-ion secondary cells. *J. Power Sources* **163**, 1003–1039 (2007).
34. Guo, J. *et al.* Interdispersed amorphous MnO_x-carbon nanocomposites with superior electrochemical performance as lithium-storage Material. *Adv. Funct. Mater.* **22**, 803–811 (2012).

35. Zheng, S. *et al.* Copper-stabilized sulfur-microporous carbon cathodes for Li–S batteries. *Adv. Funct. Mater.* **DOI**: 10.1002/adfm.201304156 (2014).
36. Shinkarev, V. V. *et al.* Sulfur distribution on the surface of mesoporous nanofibrous carbon. *Carbon* **41**, 295–302 (2003).
37. Steudel, R. Elemental sulfur and sulfur-rich compounds II. *Top. Curr. Chem.* **231**, 127–152 (2003).
38. Toniazzo, V. *et al.* Elemental sulfur at the pyrite surfaces: speciation and quantification. *Appl. Surf. Sci.* **143**, 229–237 (1999).
39. Greczynski, G. *et al.* Characterization of the PEDOT-PSS system by means of x-ray and ultraviolet photoelectron spectroscopy. *Thin Solid Film* **354**, 129–135 (1999).
40. Yang, Y. *et al.* Improving the performance of lithium-sulfur batteries by conductive polymer coating. *ACS Nano* **5**, 9187–9193 (2011).

Acknowledgments

The authors gratefully acknowledge the support of the National Science Foundation of China (No. 51272157 & 51102168). The authors would like to thank Prof. Chunsheng Wang of University of Maryland, USA for constructive suggestion.

Author contributions

S.Z. and J.Y. conceived and designed the study. S.Z. and J.Y. wrote the manuscript. S.Z., P.H. and Z.H. performed the experiments. H.Z. and Z.T. helped to do the experiments. All the authors contributed to discussion and reviewed the manuscript.

Additional information

Supplementary information accompanies this paper at http://www.nature.com/scientificreports

Competing financial interests: The authors declare no competing financial interests.

How to cite this article: Zheng, S.Y. *et al.* High Performance C/S Composite Cathodes with Conventional Carbonate-Based Electrolytes in Li-S Battery. *Sci. Rep.* **4**, 4842; DOI:10.1038/srep04842 (2014).